Control of fibrosis by TGFβ signalling modulation promotes redifferentiation during limited regeneration of mouse ear

RENÉ FERNANDO ABARCA-BUIS*,[1], MARÍA ELENA CONTRERAS-FIGUEROA[2],
DAVID GARCIADIEGO-CÁZARES[3] and EDGAR KRÖTZSCH[1]

[1]Laboratory of Connective Tissue, Centro Nacional de Investigación y Atención de Quemados, [2]Bioterio y Cirugía Experimental and [3]Unidad de Ingeniería de Tejidos, Terapia Celular y Medicina Regenerativa, Instituto Nacional de Rehabilitación Luís Guillermo Ibarra Ibarra, Mexico City, Mexico

ABSTRACT **Transforming growth factor beta (TGFβ) signalling is involved in several aspects of regeneration in many organs and tissues of primitive vertebrates. It has been difficult to recognize the role of this signal in mammal regeneration due to the low ability of this animal class to reconstitute tissues. Nevertheless, ear-holes in middle-age female mice represent a model to study the limited epimorphic-like regeneration in mammals. Using this model, in this study we explored the possible participation of TGFβ signalling in mammal regeneration. Positive pSmad3 cells, as well as TGFβ1 and TGFβ3 isoforms, were detected during the redifferentiation phase in the blastema-like structure. Daily administration of the inhibitor of the TGFβ intracellular pathway, SB431542, during 7 days from the re-differentiation phase, resulted in a decreased level of pSmad3 accompanied by a transitory higher growth of the new tissue, larger cartilage nodules, and new muscle formation. These phenotypes were associated with a decrease in the number of α-SMA-positive cells and loose packing of collagen I. These results indicate that the modulation of the fibrosis mediated by TGFβ signalling contributes to enhancing the differentiation of cartilage and muscle during limited ear-hole regeneration.**

KEY WORDS: *ear-hole, SB431542, regeneration, TGFβ signalling, fibrosis*

Introduction

Despite the amazing regenerative ability of several species of Acomys (Seifert, *et al.*, 2012; Gawriluk *et al.*, 2016), mammals usually exhibit a poor regenerative response when they sustain a traumatic injury. Notwithstanding this, although there is an incomplete closure, ear-holes in middle-age female mice show limited epimorphic regenerative features, such as rapid reepithelialization and inflammatory resolution, dermal growth similar to that of blastema-like structures, and tissue redifferentiation that conforms the ear (Reines *et al.*, 2009; Abarca-Buis *et al.*, 2017). These traits render ear-holes in middle-age female mice an accessible model to study some mechanisms underlying restrictive regeneration in mammals.

The Transforming Growth Factor beta (TGF-β) signal acts in either promoting or modulating many aspects of regeneration. Experimental administration of the inhibitor of the TGFβ signalling, SB431542, has revealed that this signal establishes and maintains the blastema through the promotion of the undifferentiated cell proliferation during the regeneration of the axolotl limb, *Xenopus* tadpole tail, and zebrafish fin (Jaźwińska *et al.*, 2007; Lévesque *et al.*, 2007; Ho and Whitman, 2008). In addition, TGFβ signal acts as an inductor of the differentiation of neural tube and notochord in *Xenopus* tail, actinotrichia in zebrafish fin, and in the epithelial-mesenchymal transition of the epidermis in the axolotl limb (Ho and Whitman, 2008; König *et al.*, 2018; Sader *et al.*, 2019). In contrast, the TGFβ signal exerts a negative effect for regeneration in other systems; during the compensatory growth of the liver, it promote fibrosis and downregulates cell proliferation in hepatocytes and hepatic progenitors (Macías-Silva *et al.*, 2002; Zhu *et al.*, 2014, Oh *et al.*, 2018) while in retinal regeneration of zebrafish and chick, TGFβ signaling inhibits proliferation and maintains the undifferentiated state of the Müller glia (Lenkowski *et al.*, 2013; Tappeiner *et al.*, 2016; Todd *et al.*, 2017). A certain notion on the role of the

Abbreviations used in this paper: α-SMA, alpha-Smooth Muscle Actin; dpw, days post-wound; dt, days of treatment; TGFβ, Transforming Growth Factor Beta; TGFβ Activated Kinase 1, TAK1; TGFβ type I Receptor, TGFβRI.

*****Address correspondence to:** René Fernando Abarca-Buis. Centro Nacional de Investigación y Atención de Quemados, Instituto Nacional de Rehabilitación Luís Guillermo Ibarra Ibarra, México, Av. México-Xochimilco No. 298, Col. Arenal de Guadalupe, Alcaldía Tlalpan, C.P.14389 Ciudad de México, México. Tel: (+52) (55) 5999 1000, exts. 14701, 14712. E-mail: buisr@yahoo.com - (iD) https://orcid.org/0000-0003-3372-813X
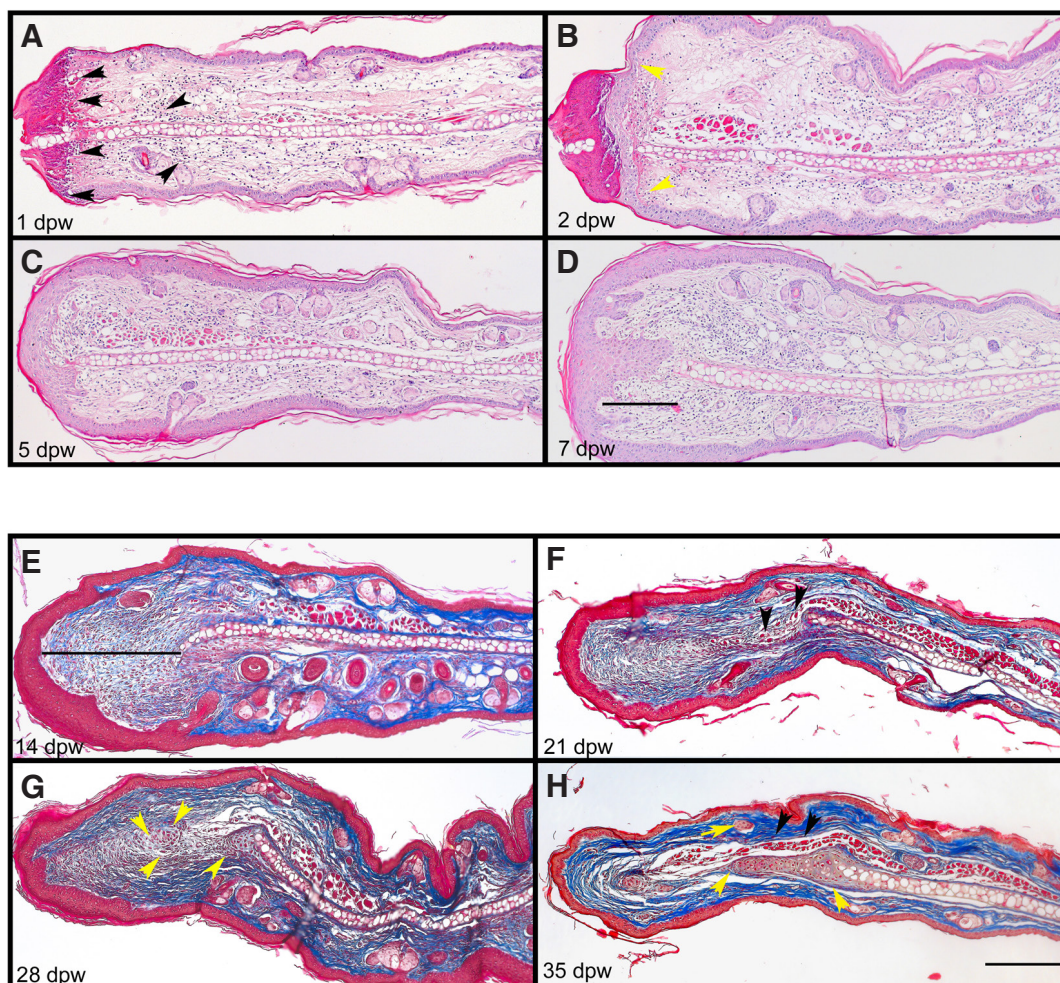
Fig. 1. Limited regeneration phases of mouse ear-hole. *Cross histological sections of middle-age female mouse ears wounded with a 2-mm thumb punch stained with H&E* **(A-D)** *at days 1* **(A)***, 2* **(B)***, 5* **(C)***, and 7* **(D)** *post-wound (dpw) or with the Masson trichrome technique* **(E-H)** *at 14* **(E)***, 21* **(F)***, 28* **(G)***, and 35* **(H)** *dpw. Black arrowheads in* **(A)** *indicate areas of inflammatory cells. Yellow arrowheads delimit the wound epidermis in* **(B)***. The line in* **(D)** *and* **(E)** *encompassing the growth of the new tissue. Black arrowheads in* **(F,H)** *point to the neo-formation of muscle. Yellow arrowheads in* **(G,H)** *indicate neo-cartilage condensation. Yellow arrow in* **(H)** *indicates a sebaceous gland formed in the neo-tissue. Scale bar, 200 μm.*

TGFβ signal in mammal regeneration has been obtained from the mouse mutagenesis induced by the adminstration of *N*-ethyl-*N*-nitrosourea. A mutation was generated with this procedure in the TGFβ type I Receptor (TGFβRI) that resulted in hyperresponsive-ness independent of ligand stimulation. The generation of a hole in the ear of these mutated mice resulted in a complete ear-hole closing with new formation of sebaceous glands, hair follicles. and islands of cartilage (Liu *et al.*, 2011). Although this experiment indicates a pro-regenerative role of the TGFβ signal in mammals, the fibrotic action is well known of TGFβ1 during wound healing and scarring using murine and human models (Shah *et al.,* 1995; Penn *et al.*, 2012; Ide *et al.,* 2017; Kanaoka *et al.,* 2018). Thus, the role of TGFβ signalling in mammalian regeneration remains unclear to date.

Making use of an ear-hole in middle-age female mice to deepen in the role of the TGFβ signal during mammalian regeneration, activation of TGFβ signaling by the presence of the transcriptional mediator, pSmad3, and the distribution of the mammalian TGFβ isoforms was determined during ear-hole repair. Mainly, the

TGFβ1 isoform and pSmad3 were associated with cells present in the blastema-like structure during the redifferentiation stage. The administration of the TGFβ signal inhibitor, SB431542, in that regenerative phase promoted dermal growth and differentiation, possibly by decreasing TGFβ fibrogenic action.

Results

TGFβ1, TGFβ3, and pSmad3 were expressed in redifferentiation phase during limited ear-hole regeneration

Three phases during the limited regeneration of the ear-hole in middle-age female mice can be identified (Fig. 1). Wound healing comprises the first evident phase and consists of the inflammatory infiltration that is notable from day 1 post-wound (Fig. 1A), a complete reepithelialisation that is evident at 2 days post-wound (dpw) (Fig. 1B), and a resolution of inflammatory infiltration from day 5 to 7 dpw (Fig. 1 C,D). In the second phase, from day 7 post-injury, the growth of new tissue is becoming apparent (Fig. 1D),

and this growth is remarkable at 14 days post-wound (dpw) (Fig. 1E). This dermal growth is similar to a blastema-like structure that harbors undifferentiated cells embedded in a loose extracellular matrix (Fig. 1E). Third, a redifferentiation phase is recognized from day 21 and involves the formation of new elastic cartilage, a thin layer of muscle localized in the dorsal region of the ear, and the formation of new pilosebaceous units (Fig. 1 F-H).

To evaluate whether the activation of TGFβ signalling is present during these different stages of the limited regeneration of mouse ear-hole, identification of pSmad3 by immunofluorescence was performed in histological sections at several dpw. pSmad3 was present in the wound-healing stage in cells that infiltrated into the injured site (Fig. 2 A-D) and was concomitantly decreased to resolution of the inflammation (Fig. 2 E-H). During the dermal growth phase, an absence of pSmad3 is evidenced (Fig. 2 I-L). Recurrence of pSmad3+ cells was observed at the beginning of the redifferentiation phase in some cells localized underlying the epidermis in the non-injured tissue at 21 dpw (Fig. 2 M,N). During the differentiation of the new tissue, pSmad3+ cells were distributed homogeneously in a blastema-like structure (Fig. 2 O,P). These results indicate that TGFβ/activin signalling is active during wound healing and the redifferentiation of the ear-hole repair.

To recognize the ligands that could activate Smad3, distribution of mammalian TGFβ isoforms were searched during ear-hole repair by immunofluorescence. TGFβ1 and TGFβ3 were detected only during the redifferentiation phase; TGFβ1 was localized in the cells of the blastema-like structure at 21 and 28 dpw (Fig. 3 A-D), while TGFβ3 was present in cells closely associated with cartilage-in-formation (Fig. 3 E-H). The TGFβ2 isoform was not detected in any stage of mouse ear-limited regeneration by this technique. TGFβ signalling has been related with the promotion of chondrogenesis through induction of the expression of Sox9, a key transcription factor that induces cartilage formation during embryogenesis (Chimal-Monroy *et al.*, 2003). To evaluate a possible correlation between TGFβ1 and TGFβ3 isoforms and the presence of Sox9, the immunodetection of Sox9 was carried out during the redifferentiation phase of limited regeneration of the ear hole. Sox9 expression was found at 28 dpw (days post-wound) (Fig. 3 I,J) and 35 dpw (Fig. 3 K,L), mainly in the cells forming cartilage condensations close to the original cartilage and after TGFβ1 and
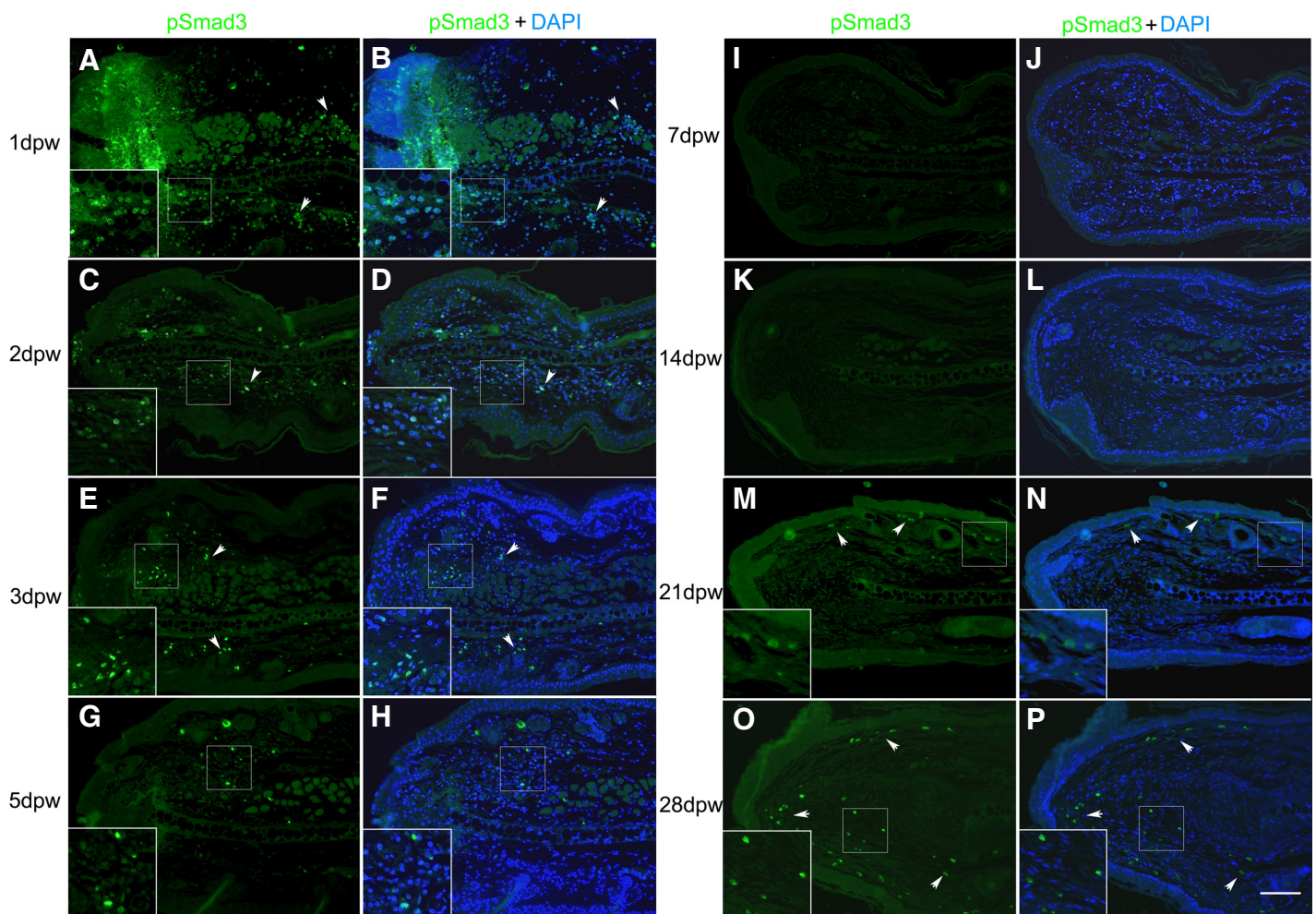
Fig. 2. Localization of pSmad3+ cells during limited regeneration of mouse ear. *Immunofluorescence of pSmad3 in cross histological sections of ears wounded with a 2-mm thumb punch at 1* **(A,B)**, *2* **(C,D)**, *3* **(E,F)**, *5* **(G,H)**, *7* **(I,J)**, *14* **(K,L)**, *21* **(M,N)** *and 28* **(O,P)** *dpw.* **(A,C,E,G,I,K,M,O)** *show pSmad3 immunolocalization (green).* **(B,D,F,H,J,L,N,P)** *show pSmad3 (green) with nuclei stained with DAPI (blue). Arrowheads indicate the presence of pSmad3 and squares indicate the digital magnification area shown in the bottom left corner Scale bar, 100 μm.*
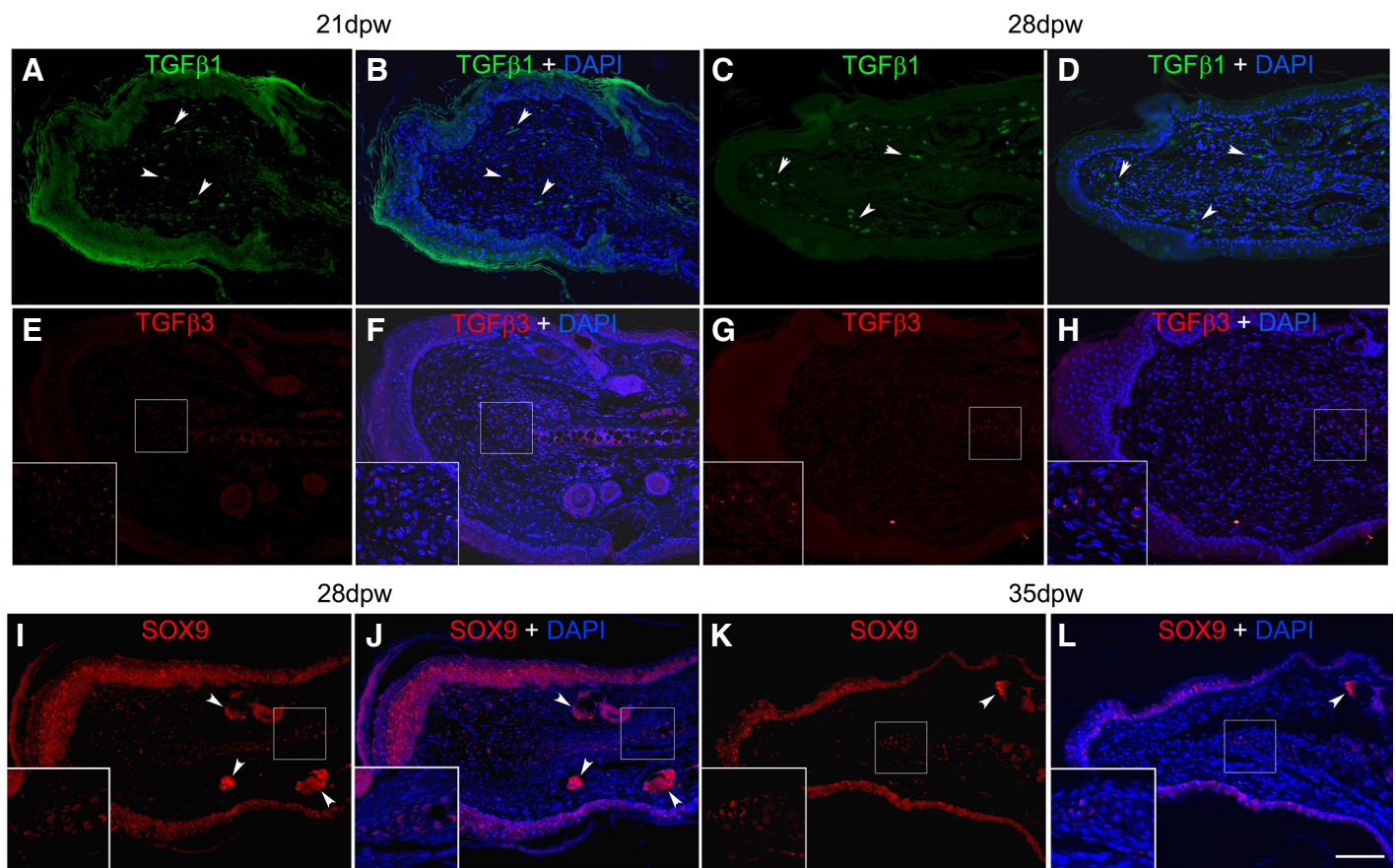
Fig. 3. TGFβ1 and TGFβ3 distribution during limited regeneration of mouse ear. (A-D) *Immunofluorescence of TGFβ1 in cross histological sections of ears wounded with a 2-mm thumb punch at 21 (**A,B**) and 28 (**C,D**) dpw. (**A,C**) shows TGFβ1 localization (green). (**B,D**) shows TGFβ1 (green) with DAPI (blue). Arrowheads indicate TGFβ1 presence. (**E-H**) Immunofluorescence of TGFβ3 at 21 (**E,F**) and 28 (**G,H**) dpw. (**E,G**) shows only the immunolocalization of TGFβ3 (red). (**F,H**) shows TGFβ3 (red) with nuclei stained with DAPI (blue). (**I-L**) Immunofluorescence of Sox9 at 28 (**I-J**) and 35 (**K,L**) dpw. (**I,K**) shows Sox9 distribution (red). (**J,L**) shows Sox9 (red) with DAPI (blue). Arrowheads indicate Sox9 in pilosebaceous units. Squares indicate the digital magnification area shown in the bottom left corner. Scale bar, 100 μm.*

TGFβ3 immunodetection. This suggested that TGFβ signalling could be involved in promoting Sox9 expression in this model. In addition, Sox9 was expressed in epidermis and pilosebaceous units (Fig. 3 I-L).

The activin β subunit and ALK4 were expressed in the wound-healing phase during limited ear-hole regeneration

pSmad3 was also observed during wound healing, but none of the TGFβ isoforms were detected by immunofluorescence during that phase. In an attempt to understand the role of the TGFβ/activin signal during wound healing, hybridization *in situ* of the *activin βb* subunit and the distribution of the activin type I receptor, ALK4, was performed during the first days post-wound. The *activin βb* subunit was expressed in wound epidermis during reepithelialization (Fig. 4 A,B), intensifying the expression as the repair progresses (Fig. 4 C,D). In a similar manner to that of pSmad3, Alk4 distribution was found in the stroma of healing tissue during inflammation (Fig. 4 E,F) and was restricted to wound epithelium at 5 and 7 dpw (Fig. 4 G,H). These observations suggest that activin diffuses from epidermis through the stroma to activate Smad3 during the wound-healing phase.

Administration of SB431542 promoted dermal growth and cartilage and muscle differentiation

Due to the presence of TGFβ1 and pSmad3 in the blastema-like structure from 21 dpw, a possible role of TGFβ signalling during the redifferentiation stage was considered. To evaluate this possibility, 2 mM of the pharmacological inhibitor of the canonical TGFβ/activin pathway, SB431542, was daily applied topically on the edge of ear-hole at 21 dpw for 7 days, while control ears were supplied with DMSO, which was used as vehicle. Treatment with the inhibitor resulted in downregulation in the ratio of pSmad3$^+$ cells in the blastema-like structure, indicating a decrease in the activity of TGFβ signalling (Fig. 5 A-D,I). We noted a significant increment in the elongation of the new tissue in ears treated with SB431542 (721.26 ± 208.89 μm) in comparison with controls (579.10 ± 135.30 μm) (Fig. 6 A-C), indicating that the modulation of TGFβ signal promotes the growth of the undifferentiated tissue and contributes to the closing of the ear-hole. To evaluate whether the downregulation of TGFβ activity affected the differentiation, the area of the chondrogenic nodules and the muscle formed *de novo* were measured. An area of <10,000 μm², corresponding to smaller cartilage nodules, was observed in 71.4% of the total cartilage
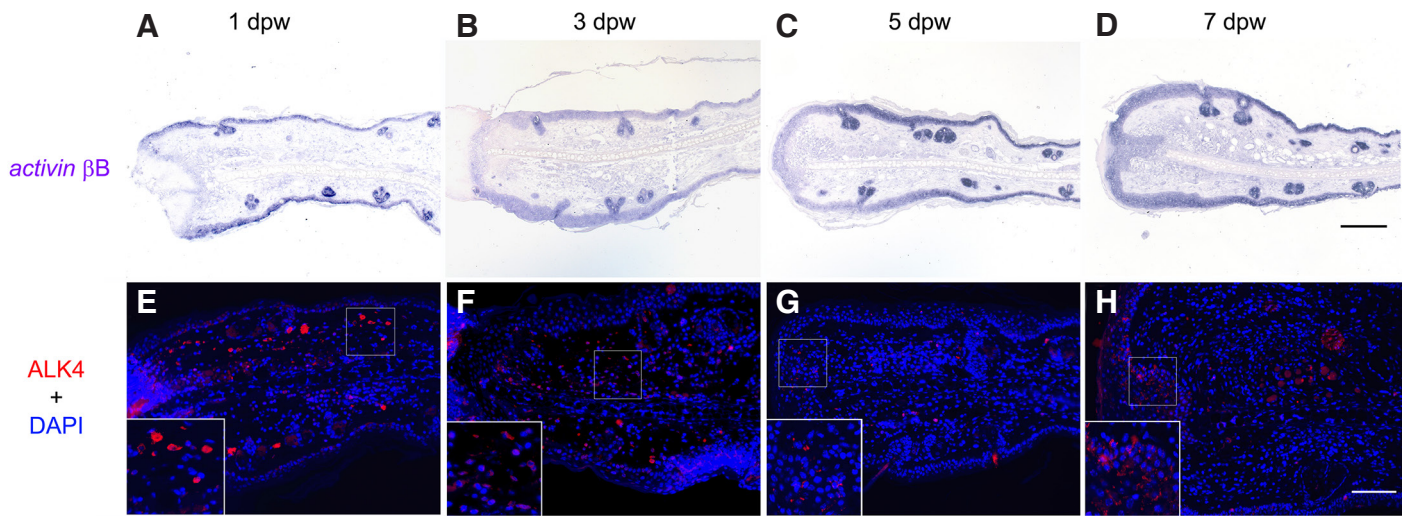
Fig. 4. Activin βb subunit expression and ALK4 distribution during wound healing phase of limited regeneration of mouse ear. (A,B) *In situ hybridization of* activin *βb subunit in cross histological sections of ears wounded with a 2-mm thumb punch at 1* **(A)**, *3* **(B)**, *5* **(C)** *and 7* **(D)** *dpw. Scale bar, 200 μm.* **(E-H)** *Immunofluorescence of ALK4 (red) with nuclei stained with DAPI (blue) at 1* **(E)**, *3* **(F)**, *5* **(G)** *and 7* **(H)** *dpw. Scale bar, 100 μm.*

nodules present in control ears, while 42.8% corresponded to cartilage nodules present in ears treated with SB431542 (*n* = 14 nodules presented in 12 sections corresponding to six ears of each group). A total of 28.6% of the control cartilage nodules fall into the interval of 10,000-30,000 μm², whereas 42.9% were observed in ears treated with the inhibitor. Large cartilage nodules of >30,000 μm² were exhibited only in ears treated with SB431542 in 14.3%

(Fig. 6 D,E). With respect to new muscle, areas of <10,000 μm² were observed in 91.6% of the controls and 58% in ears treated with the inhibitor (*n* = 12 tissue sections corresponding to six ears for each condition). A *de novo* muscle area of >20,000 μm² was exhibited in 8.3% of the control ears, while 41.6% was present in SB431542-treated ears (Fig. 6 D,E). There were no differences with respect to the number of pilosebaceous units between control and
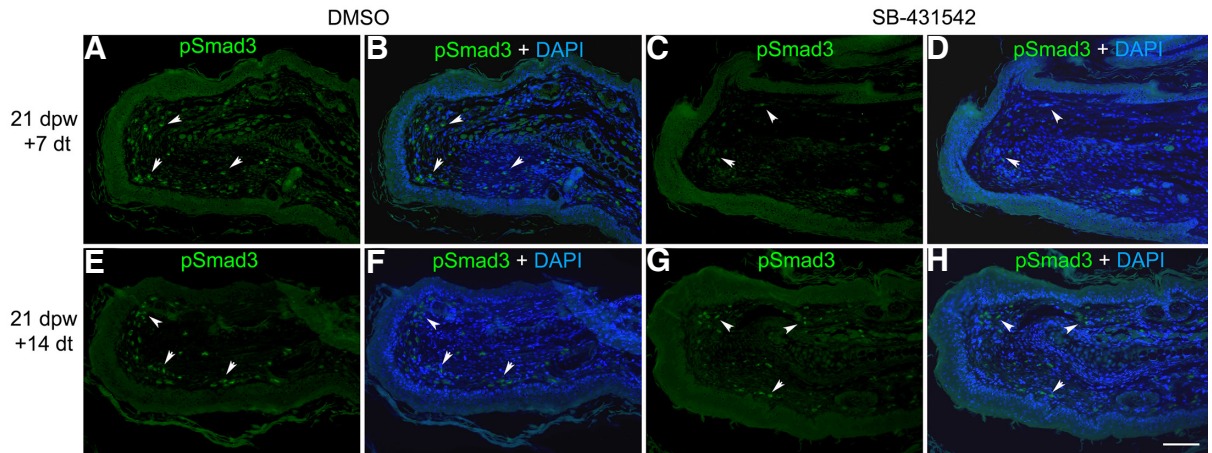
Fig. 5. pSmad3 levels in wounded ears treated with SB431542 at the redifferentiation stage. (A-D) *Presence of pSmad3+ cells in wounded ears treated with DMSO* **(A,B)** *or with SB431542* **(C,D)** *during 7 days at 21 dpw.* **(E-H)** *pSmad3+ cells in wounded ears treated with DMSO* **(E,F)** *or with SB431542* **(G,H)** *during 14 days at 21 dpw.* **(A,C,E,G)** *shows the immunolocalization of pSmad3 (green).* **(B,D,F,G)** *shows pSmad3 (green) and nuclei stained with DAPI (blue). Arrowheads indicate areas of pSmad3+ cells. Scale bar = 100 μm.* **(I)** *Graph depicting the ratio of pSmad3+ cells in the dermal new-tissue blastema-like structure of wounded ears treated with DMSO of SB431542 during 7 days (DMSO;* n *= 8 sections, SB;* n *= 10 sections) or 14 days (DMSO;* n *= 6 sections, SB431542;* n *= 10 sections).* *p = 0.028 (Student* t *test). dt, days of treatment.*
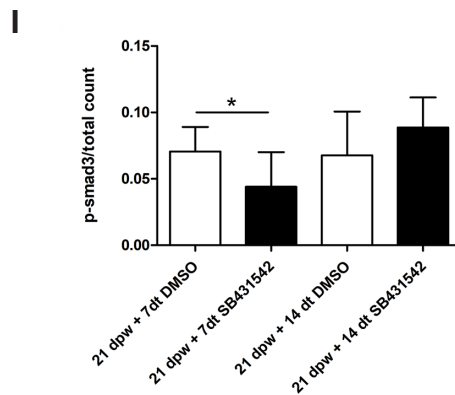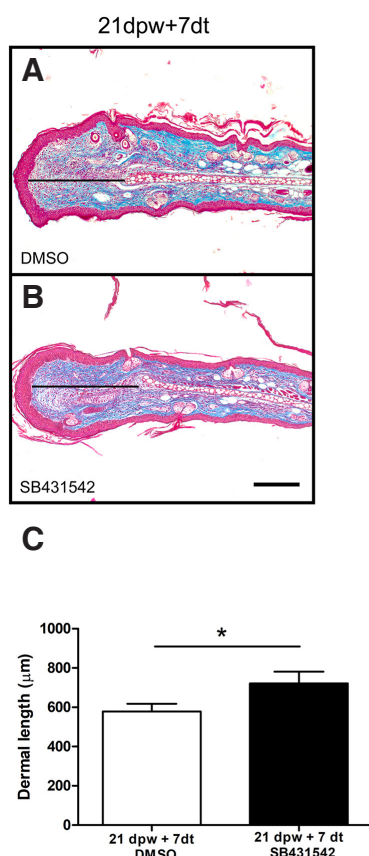
experimental conditions. The presence of larger cartilage nodules and higher neo-muscle areas in ears treated with the inhibitor indicated an improvement in the differentiation of both tissues. To evaluate the presence of cartilage progenitors in injured ears treated with SB431542, Sox9 expression by immunofluorescence was assessed. A reduction of Sox9 in both cartilages in formation and epidermis was found in ears treated with the TGFβ signal inhibitor 7 days after administration (Fig. 6 F,G), suggesting that the development of new cartilage does not depend on the inhibition of Sox9 by TGFβ signalling, but rather on mechanisms such as a reduction in fibrosis.

In order to assess whether the administration of SB exerts an effect in the short term, the ears were treated immediately with SB431542 after the wound was performed and the presence of pSmad3 was tested 1 day later. Complementarily, TGFβ1-soaked beads were implanted after the wound was performed, and the activation of Smad3 was also evaluated 1 dpw and post-bead implantation. The administration of SB431542 resulted in a decrease of Smad3 phosphorylation (Fig. 7 A,B,E,F), while an increase in the intensity of pSmad3 was evident in the ears treated with TGFβ1 (Fig. 7 C,D,G,H), indicating that the cells of mouse healing ear are responsive in a short time to TGFβ/activin signalling, which leads to a progressive effect during the differentiation stage evidenced 7 days after treatment.

Administration of SB431542 reduced fibrosis and α-SMA expression

TGFβ1 is well recognized as a profibrotic factor during the repair of several organs in mammals. On the other hand, it has been considered that fibrosis contributes to inhibiting regeneration. To evaluate whether promotion of differentiation and dermal growth by downregulation of the TGFβ signalling correlates with a decrease in fibrosis, the presence of myofibroblasts by means of the immunofluorescence of alpha-Smooth Muscle Actin (α-SMA) and collagen fiber distribution by Masson stain were analyzed in experimental and control groups. A significant reduction of α-SMA+ cells was observed in ears treated with SB431542 (Fig. 8 A-D,I). Nevertheless, only 33.3% of the ears treated with the inhibitor exhibited sparse packing of collagen. To estimate whether a prolonged treatment of SB431542 could decrease the packed packing of collagen in the neo-formed tissue, the inhibitor was administered daily during 14 days from 21 dpw. At the end of treatment, 66.6% of ears treated with SB431542 revealed a less dense packing of collagen compared to the DMSO-controls (Fig. 8 J,K). However, pSmad3 levels were not reduced in comparison to the controls after 14 days of treatment, indicating a decrease in drug absorption (Fig. 5 E-H,I). Elongation of the new tissue do not appear to have significant changes either. Although larger chondrogenic nodules and neo-muscle areas were still observed
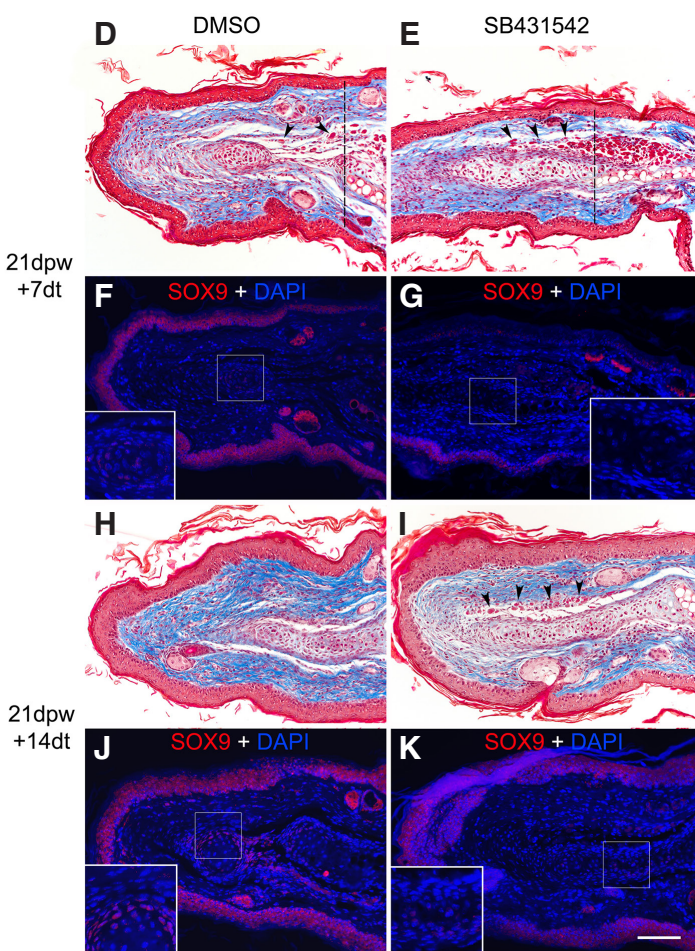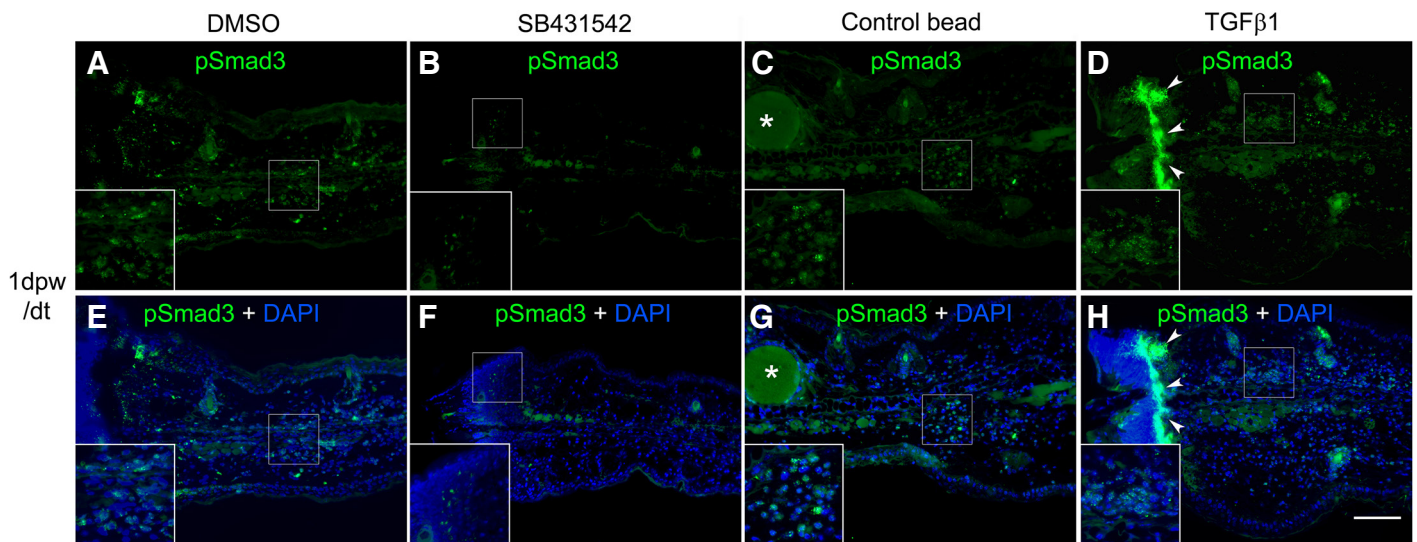

Fig. 6. The growth of the neo-formed tissue and differentiation is increased by SB431542 treatment. (A,B) *Representative images of wounded-ear edges that exhibit the length of the neo-formed tissue indicated by line extending from original cartilage to tip of the neo-formed tissue. Tissue sections were stained with the Masson trichrome technique. Scale bar = 200 µm.* **(C)** *Graph depicting the length of the neo-formed tissue in wounded ears treated with DMSO or SB431542 for 7 days (*n* = 12 sections for each condition). *p = 0.029 (Student t test).* **(D-K)** *Representative images of wounded ear edges treated with DMSO* **(D,F,H,J)** *or SB431542* **(E,G,I,K)** *for 7 days* **(D-G)** *or 14 days* **(H-K)**. **(D,E,H,I)** *Tissue sections stained with the Masson trichrome technique in which could be appreciated the cartilage nodules and the new muscle formation (arrowheads).* **(F,G,J,K)** *shows the immunolocalization of Sox9 (red) and nuclei stained with DAPI (blue). dt = days of treatment. The dashed lines in* **(D,E)** *separate the original tissue (right) from the neo-formed tissue (left). Scale bar, 100 µm.*

Fig. 7. Cells of ear healing tissue are responsive to TGFβ signal in a short term. (A-H) *Presence of pSmad3⁺ cells 1 dpw of ears treated with DMSO* **(A,E)** *SB431542* **(B,F)**, *Affi-Gel blue bead* **(C,G)** *or TGFβ1 Affi-Gel blue beads* **(D,H)** *administered immediately after wound was made.* **(A-D)** *The immunolocalization of pSmad3 (green).* **(E-H)** *pSmad3 (green) and nuclei stained with DAPI (blue). Arrowheads indicate areas of intense pSmad3⁺ signal. Asterisk indicate position of the bead. Scale bar, 100 μm. dt, days of treatment.*

in ears treated with SB431542, differences with respect to the controls were lower than when the inhibitor was administrated during 7 days: cartilage nodules of <10,000 μm² were observed in 26.7% of controls and in 25% of SB431542-treated ears, cartilage nodules from areas between 10,000 and 30,000 μm² were exhibited in 70% of controls and in 56.6% of experimental ears, and 13.3% of the controls showed cartilages >30,000 μm² whereas 18.7% of the ears treated with the inhibitor exposed this feature (Fig. 6 H,I); muscle areas of <10,000 μm² presented in 66.6% of the control ears and in 50% in SB431542- treated ears, and finally, 33.3% of the controls exhibited muscle areas of >10,000 μm², while 50% of ears treated with the inhibitor exhibited these larger muscle areas (Fig. 6 H,I). Expression of Sox9 began to be evident on the cartilage nodules of ears treated with SB431542 (Fig. 6 J,K) and changes in the rate of α-SMA⁺ cells were not significant between DMSO-controls and SB431542-treated ears during 14 days (Fig. 8 E-I). These results indicate that reduction in the packing of collagen is the consequence of the early downregulation of the TGFβ signal by SB431542 and consequently, in the decrease of α-SMA expression levels.

Discussion

In this work, we detected the expression of the *activin βb* subunit and ALK4 during the wound-healing phase and of TGFβ1 and TGFβ3 during the redifferentiation phase during the limited regeneration of the ear hole in middle-aged female mice. *Activin βb* and ALK4 expression were linked with reepithelialization and inflammation, while TGFβ3 expression was related with the chondrogenesis of elastic cartilage and TGFβ1 was associated with cells found in dermal growth with a blastema-like structure. In complementary fashion, the presence of pSmad3 in some cells present during the initial days post-wound and in the new dermal tissue indicates that the intracellular TGFβ pathway is active and suggests some role for this signal in the wound-healing and redifferentiation stages. The expression of the several TGFβ isoforms and the activation

of Smads in the blastema and buds of the different regenerative systems, such as axolotl limb, gecko tail and *Xenopus* tail (Lévesque *et al.*, 2007; Ho and Whitman, 2008; Gilbert *et al.*, 2013), suggest a role of the TGFβ signal in the redifferentiation and formation of new tissues. In fact, in loss-of-function experiments by the administration of the pharmacological inhibitor of the Smad-dependent TGFβ/activin pathway, SB431542, interfered with the formation of neural tube, notochord, and muscle during *Xenopus* tail regeneration (Ho and Whitman, 2008), inhibited the complete regeneration of axolotl limbs at the early bud stage (Lévesque *et al.*, 2007), and attenuated cardiomyocyte proliferation, altering the source of a new myocardium during the regeneration of zebrafish heart (Chablais and Jaźwińska, 2012). Contrary to those reports, in this study we found that the administration of the SB431542 starting at the redifferentiation phase during the limited regeneration of ear, transiently accelerated the growth of dermal tissue and improved the differentiation of cartilage and muscle. This finding correlated with a decrease in α-SMA expression and collagen deposition, supporting the idea that fibrosis interferes with regeneration. The blocking of regeneration by fibrosis has been evidenced by subcutaneous injection of Bleomycin during skin-wound healing in axolotl. This treatment resulted in fibrosis and the inhibition of skin regeneration (Lévesque *et al.*, 2010), and it has been suggested that slow deposition and composition of the new extracellular matrix during the wound healing of axolotl skin could promote regeneration (Seifert, *et al.*, 2012). Additionally, in accordance with our results, the reduced levels of α-SMA were also observed in the ear holes of Smad3 knockout mice that resulted in reduced wound contraction and even in enlarged excisional ear wounds due to an overexpression of elastic components (Arany *et al.*, 2006). Together with the well-recognized role of TGFβ1 as a profibrotic factor during wound healing in mammals even under pathological conditions (Sharma *et al.*, 1996; Kanzler *et al.*, 1999; Penn *et al.*, 2012; Ide *et al.*, 2017; Kanaoka *et al.*, 2018), our results indicated that TGFβ signalling promotes a fibrotic phenotype and contributes to the prevention of regeneration during late-repair in a system of
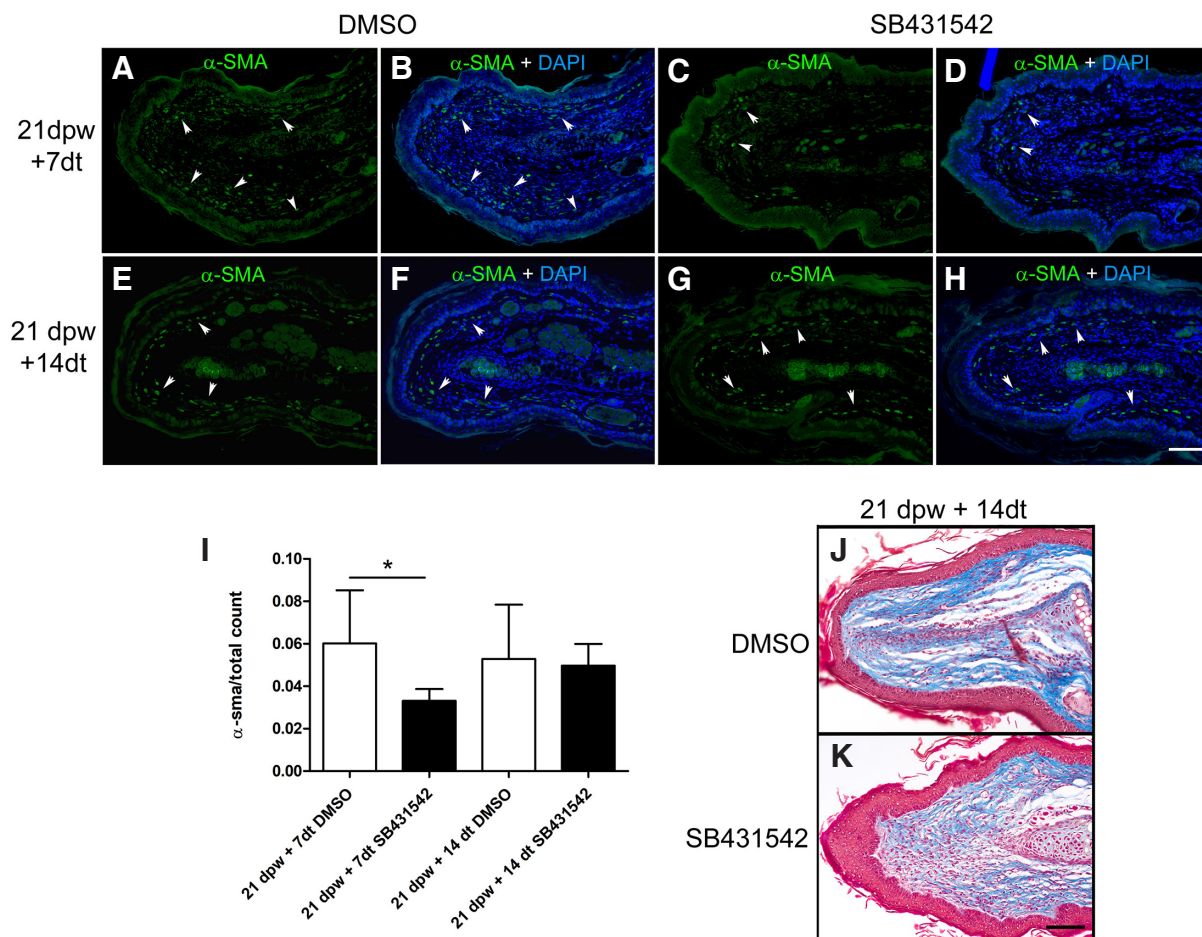
Fig. 8. Wounded ears treated with SB431542 decreased in α-SMA⁺ cells and collagen packing. (A-D) *α-SMA⁺ cells in the neo-tissue of wounded ears treated with DMSO* **(A,B)** *or SB431542* **(C,D)** *during 7 days at 21 dpw.* **(E-H)** *Presence of α-SMA⁺ cells in neo-tissue of wounded ears treated with DMSO* **(E,F)** *or SB431542* **(G,H)** *during 14 days at 21 dpw.* **(A,C,E,G)** *shows only the immunolocalization of α-SMA (green).* **(B,D,F,H)** *shows the presence of α-SMA (green) and nuclei stained with DAPI. Arrowheads indicate areas positive for α-SMA.* **(I)** *Graph depicting the rate of α-SMA⁺ cells in neo-formed tissue of wounded ears treated with DMSO or SB431542 during 7 days (DMSO; n = 6, SB431542; n = 8) and 14 days at 21 dpw (DMSO; n = 8, SB431542; n = 6).* **(J,K)** *Representative images of neo-formed tissue histological sections of wounded ears treated with DMSO* **(J)** *or SB431542* **(K)** *for 14 days and stained with the Masson trichrome technique to observe collagen packing. Scale bar, 100 μm.*

limited regenerative features in mammals.

On the other hand, contrary to our observations, a fast and regenerative healing of the ear-hole was obtained in mice with partial activation of TGFβRI, which resulted due to *N*-ethyl-*N*-nitrosourea-induced mutagenesis (Liu *et al.*, 2011). Unlike the experiment described herein, activation of TGFβRI was present throughout the wound-repair process, suggesting that early ectopic activation of TGFβ signalling could affect some events that generate a regenerative phenotype in the ear. In addition, non-canonical pathways independent of Smads could be activated to increase the regenerative response in these systems. Interestingly, it has been demonstrated that blocking the activity of TGFβ Activated Kinase 1 (TAK1), a crucial mediator of the TGFβ non-canonical pathway, resulted in the delay in wound epidermis formation during limb regeneration in axolotls, indicating a role of the non-canonical pathway in some regenerative processes (Sader *et al.*, 2019).

Although the presence of larger cartilage nodules was evident in ears treated with SB431542, a decrease on Sox9 expression,

an important inducer of chondrogenesis, was detected, pointing out that TGFβ signalling promotes Sox9 expression in the mouse healing ear in a similar manner to that occurring during development. The implantation of TGFβ1-soaked beads in the interdigit of chick-limb development induces the expression of *sox9* at 30 min after TGFβ treatment, revealing TGFβ signal as a promotor of chondrogenesis (Chimal-Monroy *et al.*, 2003). Our results are consistent with this view, although it has also been demonstrated that chondrogenesis is promoted by other mechanisms, such as the need for a loose extracellular matrix and a scar-free environment, which may be transiently obtained by a blockade of TGFβ signalling activity.

Administration of SB431542 during 14 days did not affect the levels of pSmad3, suggesting that absorption of the inhibitor decreased by extending the treatment. Notwithstanding this, the possibility is not excluded of loss of effectiveness by the drug. The daily local topical delivery of the Rho-kinase inhibitor in murine full-thickness cutaneous wounds during 12 days prevents the normal

dynamic of wound closure from day 2 to day 7 post-wound; how-ever, by day 9, no differences were found between experimental and control conditions, which may be due to changes in the bioavailability of the inhibitor (Tholpady *et al.*, 2014). The lack of effect of SB431542 administered during 14 days indicates that the decrease in tightly packed collagen is the consequence of the downregulation of α-SMA induced by early treatment with this inhibitor during the first 7 days at the beginning of the re-differentiation phase. In conclusion, these results indicate that modulation of fibrosis mediated by TGFβ signalling contributes to the differentiation of cartilage and muscle, as well as to the dermal growth of blastema-like structures.

Materials and Methods

Mice

This study was carried out in accordance with the Guide for Care and Use of Laboratory Animals of the Mexican Official Standard (NOM-062-ZOO-1999), and the protocol was approved by the Mexican Internal Committee for the Care and Use of Laboratory Animals of the Instituto Nacional de Rehabilitación Luís Guillermo Ibarra Ibarra in Mexico City. Eight-month-old female Balb-c-strain mice with an approximate weight of between 25 and 30 gr were kindly donated by the Instituto de Biotec-nología of the Universidad Nacional Autónoma de México. Animals were housed under pathogen-free conditions with food and water provided ad libitum. Vivarium conditions included the following: $21 \pm 2°C$ M $50\% \pm 10\%$ relative humidity, and a 12-h light/dark cycle.

A 2 mm diameter ear hole

The mice were anesthetized with Isoflurane (Laboratorios PiSA, Gua-dalajara, Jal., México), and a 2-mm-diameter ear hole was made in the center of the ear pinnae using a thumb punch and a piece of cardboard for support. This procedure avoids the formation of irregular wound edges, which disrupt the limited regenerative capacity of the ear (Rajnoch *et al.*, 2003). After sacrificing the mice, the ears were collected and fixed for 36 h with Protocol SAFEFIX II™ (Fisher Diagnostics, Kalamazoo, MI, USA) on days 1, 2, 3, 5, 7, 14, 21, and 28 (*n* = 4 ears/time point, two ears per animal) and processed by H&E and Masson histological stains and immunofluorescence for TGFβ1, TGFβ2, TGFβ3, pSmad3 and Sox9.

SB431542 treatment

Immediately after the ear hole was made, 20 μl of SB431542 2 mM (Abcam, cat. no. ab120163; Cambridge, UK) or DMSO (Sigma-Aldrich, cat. n. 154838-1L; St. Louis, MO, USA) was topically applied. This concentra-tion was chosen based on the effects obtained from the administration of SB431542 in subconjunctival injections in rabbit eye (Xiao *et al.*, 2009). One day after treatment, the ears were collected, fixed, and processed by pSmad3 immunofluorescence. In another group, the mice were left for 21 days and then were topically administered 20 μl of SB431542 2 mM or DMSO in the left and right ears, respectively, for 7 days. Another group was treated daily with the drug and DMSO for 14 days. Follow-ing these treatments, the ears were collected, fixed, and processed by Masson stain or by pSmad3, Sox9, and α-SMA immunofluorescence.

TGFβ1 bead implantation

Affi-Gel® Blue beads (Bio-Rad Laboratories, Hercules, CA, USA), embedded previously in a solution of 100 μg/ml recombinant human TGF-β1 (PreproTech, Inc., Rocky Hill, NJ, USA), were implanted close to the ear wounds after ear punch in 9-month-old female mice (*n* = 3 ears); beads soaked in vehicle were implanted into the opposite ear of the same animal as control. Beads were introduced using a tuberculin needle adjacent to the punch wounds. Ears were harvested and fixed at 1 day post-wound (dpw) and processed by pSmad3 immunofluorescence.

Histomorphological evaluation and immunofluorescence

Fixed ears were cut transversely through the hole; then, each ear half was dehydrated and embedded in paraffin (Paraplast®; Sigma-Aldrich, St. Louis, MO, USA). Serial cross-sections of 5-μm (Fig. 1D) were stained with H&E or Masson's trichrome. Also, tissue sections of wounded ears treated with DMSO and SB431542 were processed by immunofluores-cence. Briefly, after dewaxing and rehydration, sections were blocked and permeabilized with 1% albumin, 0.3% Triton X100 in phosphate Buffered Saline (PBS) for 2 h in room temperature and then incubated at 4°C overnight with one of the following primary antibodies: rabbit monoclonal anti-TGF beta 1 [EPR21143] (ab215715), mouse monoclonal anti-TGF beta 2 (ab36495); rabbit polyclonal anti-TGF beta 3 (ab15537); rabbit polyclonal anti-pSmad3 [phospho S425] (ab51177); rabbit polyclonal anti-Activin A Receptor Type IB (ab64813); rabbit polyclonal anti-SOX9 (ab26414) or mouse monoclonal anti-alpha smooth muscle Actin [1A4] (ab7817), all of these purchased from Abcam (Cambridge, UK). After washing, the slides were incubated at room temperature for 2 h with the following secondary antibodies: for anti-TGF beta 1 and anti-pSmad3 we used Goat Anti-Rabbit IgG H&L (Alexa Fluor® 488) (Abcam, cat. n. ab150077, Cambridge, UK), for anti-TGF beta 2 and anti-alpha smooth muscle Actin we used fluorescein $F(ab')_2$ fragment of goat anti-mouse IgG (H+L) (Invitrogen Molecular Probes, cat. n. F11021, CA, USA), and for anti-TGF beta 3, anti-ALK4 and anti-Sox9, we used DyLight®594 anti-rabbit IgG (H+L) (Vector Laboratories, cat. n. DI-1594, Burlingame, CA, USA). Sections were washed three times in PBS with 0.3% Triton and then twice in PBS, followed by mounting with Vectashield® containing 4',6-DiAmino-2-PhenylIndole (DAPI; Vector Laboratories, Burlingame, CA, USA) and cover slipping.

Activin βb in-situ hybridization

Tissue sections of wounded ears were hydrated through graduated methanols until PBT, post-fixed with cold PFA 4% during 15 min, and treated with 1 μg/ml proteinase K (preincubated at 37°C) for 5 min at room temperature, then washed with PBT and pre-incubated with hybridization buffer at 55°C for 15 min. After this, tissue sections were incubated with the *activin βB* probe overnight and washed with a solution of formamide 50%, SSC 4X, SDS 1%, and a solution with formamide 50%, SSC 2X 3 times during 15 min at 50°C for each section. Washes with TBST + 2 mM Levamisole hydrochloride 2 mM (Sigma-Aldrich, St. Louis, MO, USA) were carried out and the sections were blocked with 10% goat serum during 30 min, incubated with anti-DIG-AP (Roche Diagnostics GmbH, Mannheim, Germany), and diluted 1:500 overnight at 4°C. Sec-tions were washed with TBST + Levamisole 2 mM and NTMT + 1 mM Levamisole and revealed with BM-Purple (Roche Diagnostics GmbH, Mannheim, Germany).

Image acquisition and morphometric analysis

Tissue sections were captured using an Imager Z1 microscope (Carl Zeiss). For bright-field and fluorescent image acquisition, high-speed polychromatic and monochromatic cameras (AxioCam; Carl Zeiss), respectively, were used. Measures of chondrogenic and muscle areas, as well as the elongation of the dermal growth, were performed using AxioVision software (ver. 4.8.1.0; Carl Zeiss) on the images acquired.

Statistical analyses

Statistical analyses were carried out using GraphPad Prism ver. 8 statistical software. D'Agostino & Pearson and Shapiro-Wilk normality tests were utilized to data distribution. Normally distributed data were analyzed by the two-tailed Student *t* test. Data are expressed as the mean ± Standard Deviation (SD) *P* values ≤0.05 were considered significant.

References

ABARCA-BUIS RF, MARTÍNEZ-JIMÉNEZ A, VERA-GÓMEZ E, CONTRERAS-FIGUEROA ME, GARCIADIEGO-CÁZARES D, PAUS R, ROBLES-TENORIO A, KRÖTZSCH E (2017). Mechanisms of epithelial thickening due to IL-1 signalling blockade and TNF-α administration differ during wound repair and regeneration. *Differentiation* 99: 10–20.

ARANY PR, FLANDERS KC, KOBAYASHI T, KUO CK, STUELTEN C, DESAI KV, TUAN R, RENNARD SI, ROBERTS AB (2006). Smad3 deficiency alters key structural elements of the extracellular matrix and mechanotransduction of wound closure. *Proc. Natl. Acad. Sci. USA* 103: 9250–9255.

CHABLAIS F, JAŹWIŃSKA A (2012). The regenerative capacity of the zebrafish heart is dependent on TGFβ signaling. *Development* 139: 1921–1930.

CHIMAL-MONROY J, RODRIGUEZ-LEON J, MONTERO JA, GAÑAN Y, MACIAS D, MERINO R, HURLE JM (2003). Analysis of the molecular cascade responsible for mesodermal limb chondrogenesis: Sox genes and BMP signaling. *Dev Biol* 257: 292-301.

GAWRILUK TR, SIMKIN J, THOMPSON KL, BISWAS SK, CLARE-SALZLER Z, KIMANI JM, KIAMA SG, SMITH JJ, EZENWA VO, SEIFERT AW (2016). Comparative analysis of ear-hole closure identifies epimorphic regeneration as a discrete trait in mammals. *Nat Commun* 7: 11164.

GILBERT RWD, VICKARYOUS MK, VILORIA-PETIT AM (2013). Characterization of TGFβ signaling during tail regeneration in the leopard Gecko (*Eublepharis macularius*). *Dev Dyn* 242: 886–896.

HO DM, WHITMAN M (2008). TGF-beta signaling is required for multiple processes during *Xenopus* tail regeneration. *Dev. Biol* 315: 203–216.

IDE M, JINNIN M, TOMIZAWA Y, WANG Z, KAJIHARA I, FUKUSHIMA S, HASHIZUME Y, ASANO Y, IHN H (2017). Transforming growth factor β inhibitor Repsox downregulates collagen expression of scleroderma dermal fibroblasts and prevents Bleomycin-induced mice skin fibrosis. *Exp Dermatol* 26: 1139–1143.

JAŹWIŃSKA A, BADAKOV R, KEATING MT (2007). Activin-βA signaling is required for zebrafish fin regeneration. *Curr Biol* 17: 1390–1395.

KANAOKA M, YAMAGUCHI Y, KOMITSU N, FEGHALI-BOSTWICK CA, OGAWA M, ARIMA K, IZUHARA K, AIHARA M (2018). Pro-fibrotic phenotype of human skin fibroblasts induced by periostin via modulating TGF-β signaling. *J Dermatol Sci* 90: 199–208.

KANZLER S, LOHSE AW, KEIL A, HENNINGER J, DIENES HP, SCHIRMACHER P, ROSE-JOHN S, BÜSCHENFELDE ZUM KH, BLESSING M (1999). TGF-beta1 in liver fibrosis: an inducible transgenic mouse model to study liver fibrogenesis. *Am J Physiol* 276: G1059–G1068.

KÖNIG D, PAGE L, CHASSOT B, JAŹWIŃSKA A (2018). Dynamics of actinotrichia regeneration in the adult zebrafish fin. *Dev Biol* 433: 416–432.

LENKOWSKI JR, QIN Z, SIFUENTES CJ, THUMMEL R, SOTO CM, MOENS CB, RAYMOND PA (2013). Retinal regeneration in adult zebrafish requires regulation of TGFβ signaling. *Glia* 61: 1687–1697.

LÉVESQUE M, GATIEN S, FINNSON K, DESMEULES S, VILLIARD E, PILOTE M, PHILIP A, ROY S (2007). Transforming growth factor: beta signaling is essential for limb regeneration in axolotls. *PLoS One* 2: e1227.

LÉVESQUE M, VILLIARD E, ROY S (2010). Skin wound healing in axolotls: a scarless process. *J Exp Zool* 314B: 684–697.

LIU J, JOHNSON K, LI J, PIAMONTE V, STEFFY BM, HSIEH MH, NG N, ZHANG J, WALKER JR, DING S, MUNEOKA K, WU X, GLYNNE R, SCHULTZ PG (2011). Regenerative phenotype in mice with a point mutation in transforming growth factor beta type I receptor (TGFBR1). *Proc Natl Acad Sci USA* 108: 14560–14565.

MACÍAS-SILVA M, LI W, LEU JI, CRISSEY MA, TAUB R (2002). Up-regulated transcriptional repressors SnoN and Ski Bind Smad proteins to antagonize transforming growth factor-β signals during liver regeneration. *J Biol Chem* 277: 28483–28490.

OH S-H, SWIDERSKA-SYN M, JEWELL ML, PREMONT RT, DIEHL AM (2018). Liver regeneration requires Yap1-TGFβ-dependent epithelial-mesenchymal transition in hepatocytes. *J Hepatol* 69: 359–367.

PENN JW, GROBBELAAR AO, ROLFE KJ (2012). The role of the TGF-β family in wound healing, burns and scarring: a review. *Int J Burns Trauma* 2: 18–28.

RAJNOCH C, FERGUSON S, METCALFE AD, HERRICK SE, WILLIS HS, FERGUSON MWJ (2003). Regeneration of the ear after wounding in different mouse strains is dependent on the severity of wound trauma. *Dev Dyn* 226: 388–397.

REINES B, CHENG LI, MATZINGER P (2009). Unexpected regeneration in middle-aged mice. *Rejuv Res* 12: 45–52.

SADER F, DENIS J-F, LAREF H, ROY S (2019). Epithelial to mesenchymal transition is mediated by both TGF-β canonical and non-canonical signaling during axolotl limb regeneration. *Sci Rep* 9: 1144.

SEIFERT AW, KIAMA SG, SEIFERT MG, GOHEEN JR, PALMER TM, MADEN M (2012). Skin shedding and tissue regeneration in African spiny mice (*Acomys*). *Nature* 489: 561–565.

SEIFERT AW, MONAGHAN JR, VOSS SR, MADEN M (2012). Skin Regeneration in adult axolotls: a blueprint for scar-free healing in vertebrates. *PLoS One* 7: e32875–e32919.

SHAH M, FOREMAN DM, FERGUSON M (1995). Neutralisation of TGF-beta 1 and TGF-beta 2 or exogenous addition of TGF-beta 3 to cutaneous rat wounds reduces scarring. *J Cell Sci* 108: 985–1002.

SHARMA K, JIN Y, GUO J, ZIYADEH FN (1996). Neutralization of TGF-β by anti-TGF-β antibody attenuates kidney hypertrophy and the enhanced extracellular matrix gene expression in STZ-induced diabetic mice. *Diabetes* 45: 522–530.

TAPPEINER C, MAURER E, SALLIN P, BISE T, ENZMANN V, TSCHOPP M (2016). Inhibition of the TGFβ pathway enhances retinal regeneration in adult zebrafish. *PLoS One* 11: e0167073.

THOLPADY SS, DEGEORGE BR, CAMPBELL CA (2014). The effect of local rho-kinase inhibition on murine wound healing. *Ann Plast Surg* 72: S213–S219.

TODD L, PALAZZO I, SQUIRES N, MENDONCA N, FISCHER AJ (2017). BMP- and TGFβ-signaling regulate the formation of Müller glia-derived progenitor cells in the avian retina. *Glia* 65: 1640–1655.

XIAO Y-Q, LIU K, SHEN J-F, XU G-T, YE W (2009). SB-431542 Inhibition of scar formation after filtration surgery and its potential mechanism. *Invest Ophthalmol Vis Sci* 50: 1698–1699.

ZHU Z, CHEN J, XIONG J-W, PENG J (2014). Haploinsufficiency of Def activates p53-dependent TGFβ signalling and causes scar formation after partial hepatectomy. *PLoS One* 9: e96576–e96613.

Further Related Reading, published previously in the *Int. J. Dev. Biol.*

Nerve roles in blastema induction and pattern formation in limb regeneration
Akira Satoh, Kazumasa Mitogawa and Aki Makanae
Int. J. Dev. Biol. (2018) 62: 605-612

Rebuilding a planarian: from early signaling to final shape
Francesc Cebrià, Teresa Adell and Emili Saló
Int. J. Dev. Biol. (2018) 62: 537-550

Linking wound response and inflammation to regeneration in the zebrafish larval fin
Henry Hamilton Roehl
Int. J. Dev. Biol. (2018) 62: 473-477

An integrative framework for salamander and mouse limb regeneration
Duygu Payzin-Dogru and Jessica L. Whited
Int. J. Dev. Biol. (2018) 62: 393-402

The evolution of regeneration – where does that leave mammals?
Malcolm Maden
Int. J. Dev. Biol. (2018) 62: 369-372

External ear microRNA expression profiles during mouse development
Leda Torres, Ulises Juárez, Laura García, Juan Miranda-Ríos and Sara Frias
Int. J. Dev. Biol. (2015) 59: 497-503
https://doi.org/10.1387/ijdb.150124sf

From Planarians to Mammals - the many faces of regeneration
Jerzy Moraczewski, Karolina Archacka, Edyta Brzoska, Maria-Anna Ciemerych, Iwona Grabowska, Katarzyna Janczyk-Ilach, Wladyslawa Streminska and Malgorzata Zimowska
Int. J. Dev. Biol. (2008) 52: 219-227